Solvent Effect in Liquid-Phase Hydrogenation of Toluene

Petri A. Rautanen,* Juhani R. Aittamaa, and A. Outi I. Krause

Department of Chemical Technology, Helsinki University of Technology, P.O. Box 6100, FIN-02015 HUT, Finland

Liquid-phase hydrogenation of toluene in isooctane, *n*-heptane, and cyclohexane was studied on a commercial Ni/Al$_2$O$_3$ catalyst at 100−200 °C and 20−40 bar. None of the solvents was adsorbed on the catalyst. The variation in the hydrogenation rates is explained by the variation in the hydrogen solubility: the reaction rates in isooctane and *n*-heptane were similar, whereas the reaction rate in cyclohexane was lower, especially at higher temperatures. The reaction order for toluene was close to 0, while the reaction order with respect to hydrogen increased from near 0 to 1 with increasing temperature. A kinetic model based on the multiplet theory describes well the reaction orders and gives a good fit with physically reasonable parameters.

1. Introduction

Tightening legislation in regards to vehicle exhaust emissions has forced the industry to improve motors and catalytic converters and also the quality of fuels. Lead-free and low-sulfur fuels have been introduced and CO, SO$_x$, and NO$_x$ emissions have been significantly reduced. The major concern remaining is particle emissions.[1] Particles are reported[2] to correspond to aromatic compounds, and the reduction of these is the next target. The faster growth in the demand for diesel fuel relative to gasoline, together with today's higher quality requirements and lower grade raw materials, creates a need for improved dearomatization processes.[3] Better knowledge of reactions and rigorous reactor and kinetic models is essential to new process development and optimization.

Gas-phase dearomatization has been widely studied, both on metal sulfides (Co/Ni and Mo/W) and on group VIII metals (Pt, Pd, Ni, and Ru).[4] Publications on liquid-phase reaction kinetics, in turn, are few,[3,5] even though industrial dearomatization takes place in the liquid phase in three-phase reactors. Another problem is that modeling studies are usually performed with pure aromatic compounds, in the absence of solvent, whereas industrial units treat aromatic feeds in hydrocarbon mixtures.

Despite the vast amount of research, no consensus exists about the hydrogenation mechanism of the aromatic ring. Zero-order reaction of aromatics and close to first-order reaction of hydrogen are frequently reported.[6] A maximum in the reaction rate as a function of temperature is also often obtained in dearomatization.[7−11] Hydrogenation products typically contain cyclohexane, seldom cyclohexene, and there is no report of cyclohexadiene. Cyclohexadiene has nevertheless been postulated to be a reaction intermediate,[3,6−10,12] though it is thermodynamically unfavorable.[13,14] This reaction step is explained in terms of kinetic coupling;[15] i.e., the next steps are so fast that they pump down the cyclohexadiene content. The theory of kinetic coupling has also been criticized[14] and an alternative mechanism is suggested, where intermediates retain their aromatic nature according to the multiplet theory.[11,13,14] An adsorbed aromatic compound is explained to form a complex with the catalyst surface atoms and hydrogen. This complex is isomerized to cyclohexene and, thus, the formation of thermodynamically unfeasible cyclohexadiene is not included in the reaction mechanism.[14]

Hydrocarbon feed to a dearomatization unit typically contains 10−40% of aromatic compounds, while the rest consists mainly of alkanes, cycloalkanes, and alkenes. In this work, in which a more realistic model of hydrogenation was sought, toluene was used as the model aromatic compound and the hydrogenation rate was evaluated in three solvents selected to represent nonaromatic components. These were straight chain alkanes (*n*-heptane), branched alkanes (isooctane), and cycloalkanes (cyclohexane).

2. Experimental Section

2.1. Catalyst and Materials. A commercial Ni/Al$_2$O$_3$ catalyst (Ni, 16.6 wt %; specific surface area, 108 m^2/g; mean pore volume, 0.37 cm^3/g; bulk density, 0.86 g/cm^3) was crushed to 0.5−0.6 mm size. Before the hydrogenation it was pretreated by drying at 110 °C in nitrogen flow and then reduced in situ in hydrogen at 325 °C with vigorous stirring for 2 h. The reduction was performed with a pure hydrogen flow of 200 cm$^3_{NTP}$/min at atmospheric pressure. A fresh catalyst was used in each experiment, and the pretreatment procedure was automated in order to ensure a reproducible activation.

Isooctane (>99.5%), *n*-heptane (>99%), cyclohexane (>99.5%), and toluene (>99.7%) obtained from Riedel−de Haën and hydrogen (>99.999%) and nitrogen (>99.9999%) obtained from AGA were used as received.

2.2. Hydrogenation. Hydrogenation of toluene was performed in a Robinson−Mahoney-type, fixed catalyst basket reactor working isothermally in the CSTR mode. The reactor volume was 50 cm^3, and the liquid volume was defined by the step response method. The reactor was equipped with a magnetic stirrer, and the agitation speed was controlled with a frequency transformer. The reactor temperature was regulated (±0.5 °C) with a programmable temperature controller. The gas outlet flow was controlled in order to keep the desired pressure level (±0.1 bar) in the reactor. Liquid and gas feed flow

* To whom correspondence should be addressed. Fax: +358-9-4512622. E-mail: Petri.rautanen@hut.fi.

rates were controlled by mass flowmeters. Liquid and gas products were withdrawn and separated in a flash unit. The liquid level in the flash unit was regulated with an ultrasonic level controller. Liquid products were analyzed with a gas chromatograph (GC), fused silica capillary column, and flame ionization (FI) detector. The GC was equipped with an online liquid sampling valve. The GC signal was monitored and processed by a computer.

Several start-up procedures were tested without significant differences in reaction rates. The temperature and pressure were increased under a nitrogen atmosphere during the start-up. The temperature was varied from 100 to 200 °C, and the pressure was increased at higher temperatures to avoid evaporation. The toluene concentration was varied from 15 to 35 mol %. Mass-transfer experiments were performed at fixed temperature (100 °C) and pressure (20 bar) and a toluene concentration of 25 mol %. The liquid flow rate was 50 g/h (LHSV of about 3.8 h^{-1}) and the hydrogen flow 258 cm$^3_{NTP}$/min, which corresponds to the initial hydrogen to toluene molar ratio of 6:1 (toluene concentration, 25 mol %). The conversion of toluene was always kept far below the thermodynamic equilibrium conversion, which was close to 100% under the studied conditions.

3. Results and Discussion

3.1. Mass Transfer. The mass transfer of the sparingly soluble hydrogen is frequently the rate-determining step in liquid-phase hydrogenation. Hydrogen is first dissolved through the gas−liquid (GL) interface and then transferred through the liquid bulk to the liquid−solid (LS) interface. Thereafter, it is transferred through the LS interface and the catalyst pores and adsorbed on active sites on the catalyst, where the reaction finally takes place. Proper determination of the catalyst activity and kinetics requires that these mass-transfer resistances are taken into consideration in the determination of the kinetic parameters.

The mass transfer at the GL interface occurs in both directions: from gas to liquid and vice versa. However, thermodynamic vapor−liquid equilibrium (VLE) calculations [Soave−Redlich−Kwong (SRK) equation of state] showed that the major liquid compounds (toluene, solvents, and reaction products) were virtually nonvolatile because of the high pressure. Therefore, the mass-transfer resistance existed only at the liquid film, and only the hydrogen mass transfer could limit the reaction rate (pure hydrogen was used) at the GL interface. Molar fluxes at the liquid film were related to the diffusion fluxes, J_i.

$$N_{GL,i} = J_{GL,i} + N_{tot}x_i \qquad (1)$$

$$J_{GL,i} = k_{L,i}c_{tot}(x^i_{L,i} - x^b_{L,i}) \qquad (2)$$

The volumetric liquid-side mass-transfer coefficients, $k_{L,i}$, were obtained with the correlation of Miller[16] and the molar flux of hydrogen, N_{GL,H_2}, with the observed reaction rate ($N_{GL,i} = 0$ for other components). The calculated difference in hydrogen concentration over the liquid-side film, $(x^i_{L,H_2} - x^b_{L,H_2})/(x^b_{L,H_2})$, was about 2%, indicating that the hydrogen mass-transfer resistance was negligible.
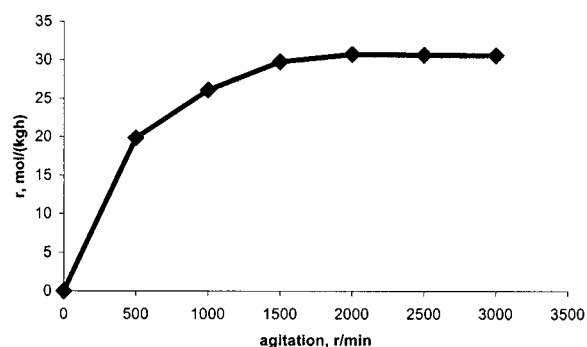

Figure 1. Effect of agitation on the reaction rate (toluene 25 mol %, 100 °C, 20 bar).
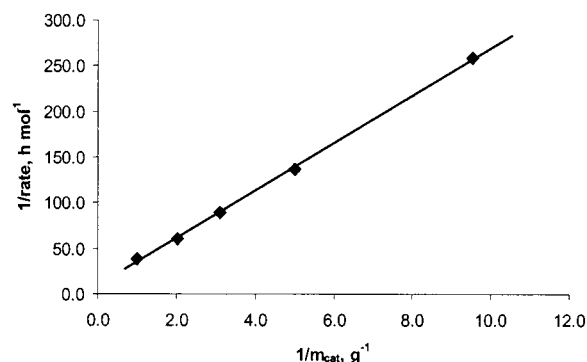

Figure 2. Effect of catalyst loading on the reaction rate (toluene 25 mol %, 100 °C, 20 bar).
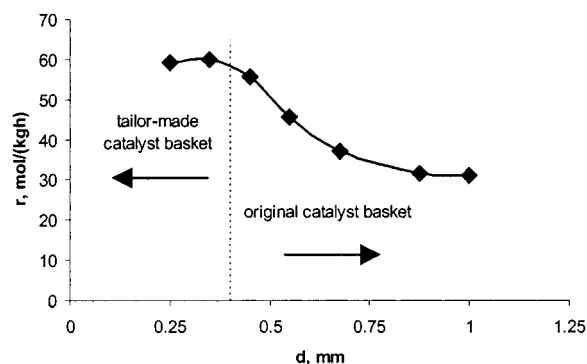

Figure 3. Reaction rate as a function of catalyst particle size (toluene 25 mol %, 100 °C, 20 bar).

The GL and LS mass-transfer resistances were also determined experimentally by varying the agitation and the catalyst loading. The hydrogenation rate as a function of stirring speed, ω, is illustrated in Figure 1. The rate increased with ω and reached a plateau when $\omega \geq 2000$ rpm. This indicates that, at low agitation, the reaction rate was limited by external mass transfer (GL and LS), but with increased agitation, the mass-transfer resistance vanished. The absence of bulk diffusion limitations is also seen as a linear dependence of the reciprocal of the hydrogenation rate versus the reciprocal of the catalyst loading (see Figure 2).[20]

Experiments with various particle sizes showed the difficulty of avoiding intraparticle mass-transfer resistances (Figure 3). In fact, it was not possible to achieve a situation in which the diffusion did not have an effect on the hydrogenation rate. A new catalyst basket was accordingly made with a smaller screen opening to allow the use of smaller catalyst particles. A problem of LS mass-transfer resistance arose with the new screen, and because it proved impossible to remove

this resistance with the available agitator, the original catalyst basket and catalyst nominal size of 0.55 mm were used. This setup ensured the absence of mass-transfer limitation at least from the liquid to the catalyst surface. The calculated Weisz–Prater criterion[17] based on the rate of hydrogen consumption was $\Phi = 31$, indicating strong diffusion limitation.

The hydrogenation of aromatics is an exothermic reaction, and because of the intraparticle diffusion, it was necessary to evaluate the heat-transfer resistance within the catalyst. Toppinen et al.[4] have reported very mild heat-transfer resistance for aromatic liquid-phase hydrogenation despite the severe mass-transfer resistance in the catalyst. Indeed, the calculated maximum temperature difference (in the catalyst particle), according to Damkoehler's criterion,[18] was only 0.6 °C and, therefore, heat transfer was assumed to be fast (isothermal) in the reactor model.

The agitation speed (2500 rpm) and the catalyst loading (<0.1 g) for the kinetic experiments were selected to avoid mass-transfer resistance at the GL and LS interfaces. The model of the intraparticle mass transfer was included in the reactor model, while the intraparticle heat-transfer resistance was neglected. These measures ensured a proper determination of the kinetic parameters independently of the mass-transfer parameters.

3.2. Reactor Model. The reactor model consisted of mass balances for the bulk gas and liquid and a balance for the interior of the catalyst particle. The mole balances for the gas and liquid phases were

$$F_{G,i0} = F_{G,i} + V_R N_{GL,i} a_{GL} \tag{3}$$

$$F_{L,i0} + V_R N_{GL,i} a_{GL} = F_{L,i} + m_{cat} r_{i,app} \tag{4}$$

and inside the catalyst particle

$$\frac{D_{i,eff}}{\epsilon R_p^2}\left(\frac{\partial^2 c_i}{\partial x^2} + \frac{2}{x}\frac{\partial c_i}{\partial x}\right) + r_i \frac{\rho_p}{\epsilon} = 0 \tag{5}$$

with boundary conditions

$$c_{L,i}^b = c_{L,i}^p$$

at $x = 1$ (at the outer surface of the catalyst)

$$\left.\frac{\partial c}{\partial x}\right|_{x=0} = 0 \qquad \text{at the center of the catalyst}$$

The apparent reaction rate (or flux) at the catalyst surface was then

$$r_{i,app} = \frac{3 D_{i,eff}}{R_p^2 \rho_p}\left.\frac{\partial c_i}{\partial x}\right|_{x=1} \tag{6}$$

The effective diffusion coefficient was computed from eq 7. The diffusion coefficients were calculated from

$$D_{i,eff} = \frac{\epsilon}{\tau} D_i \tag{7}$$

Wilke's equation.[19] Average values were used for porosity (0.5) and tortuosity (4.0),[20] whereas the catalyst density was experimentally defined (2300 kg/m³). The mass transfer at the GL interface was described in section 3.1.
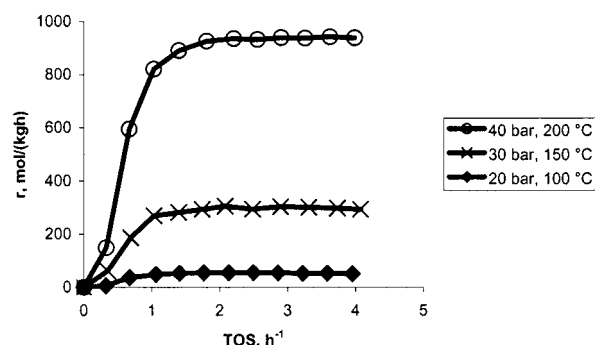

Figure 4. Toluene (25 mol %) hydrogenation rate in isooctane as a function of time on stream (TOS).
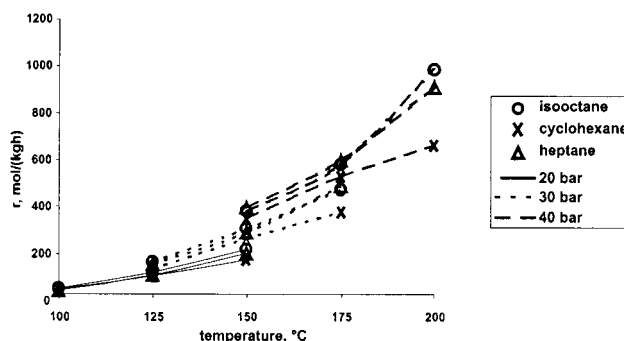

Figure 5. Toluene (25 mol %) hydrogenation in isooctane, *n*-heptane, and cyclohexane at different pressures and temperatures.

Low flow rates ($\sim 10^{-4}$ mol/s) together with large concentration values ($\sim 10^2 - 10^3$ mol/m³) caused numerical problems, which were solved by using mole fractions of bulk phases and total mole flow as variables instead of mole flows of individual components. Relative component concentrations (relative to liquid bulk) inside the catalyst were also used. Furthermore, a summary equation for bulk mole fractions ($\sum x_i = 1$) was added to the reactor model.

An ordinary partial differential equation for the mass balance inside a catalyst particle was discretized by a five-point central difference formula. Nonlinear algebraic balance equations, eqs 3, 4, and discretized 5, were solved with the Newton–Raphson method. The reactor model was integrated in a FLOWBAT flowsheet simulator,[21] which included a databank of thermodynamic properties as well as VLE calculation procedures and mathematical solvers.
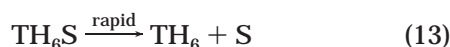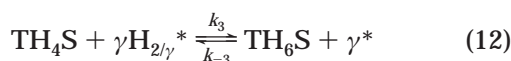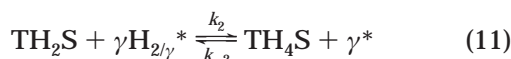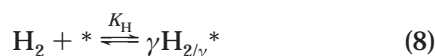
3.3. Hydrogenation, Qualitative Results. Steady state of the reactor system, including the reactor, the GL separator, and the pipe lines, was achieved after 1.5 h, and the average reaction rate was measured during the next 2 h. Typical runs are presented in Figure 4, which reveals that no decline in activity occurred during the experiments. Methylcyclohexane was the only reaction product detected; no traces of methylcyclohexene or methylcyclohexadiene were found. The hydrogenation rate increased with temperature and hydrogen pressure (Figure 5). No maximum in the rate was observed between 100 and 200 °C, though such maxima are frequently reported in the gas-phase dearomatization with group VIII metals.[5,7–11] One explanation of the maximum in the reaction rate was the variation in the hydrogen or aromatic adsorption with temperature (desorption being dominant at higher temperatures).[5,7] The maximum in the reaction rate is also observed to shift to higher temperature when the hydrogen pressure

is increased.[9,11] In the liquid phase, increased hydrogen solubility at higher temperatures and pressures led to a higher concentration of hydrogen at the catalyst surface and to an increased hydrogenation rate. This compensated the effect of the hydrogen desorption and/ or shifted the reaction rate maximum to a higher temperature and thus led to a continuously increasing reaction rate in the temperature range studied, as illustrated in Figure 5.

The type of solvent did not have a significant effect on the hydrogenation rate at 20 bar. Only minor deviations were noticed at 150 °C. At 30 bar the rates were equal in *n*-heptane and isooctane but considerably lower in cyclohexane. At 40 bar the difference was more pronounced because of the higher temperature. The differences in the reaction rates in the solvents at higher temperatures are of the same order of magnitude as the differences in the calculated (SRK equation of state) equilibrium solubility of hydrogen in the solvents. The solubility of hydrogen in cyclohexane is about 40% lower than the solubility of hydrogen in *n*-heptane and iso-octane (Figure 6).

The apparent reaction order of toluene was close to 0, and the reaction order of hydrogen increased from near 0 to 1 with increasing temperature. Similar orders have been reported, and they are often related to the strong adsorption of the aromatic compound.[6] Note, however, that comparison is not straightforward because, in our work, pressure was not constant through the entire temperature range.

3.4. Hydrogenation Kinetics. Two mechanisms based on multiplet theory were applied. It was assumed that the adsorbed aromatic compound formed an aromatic-type complex with hydrogen and two catalyst atoms. The principle of the complex formation is illustrated in Figure 7. The experimental data were first modeled with the mechanism described by Smeds et al.[11] (originally derived for the gas-phase hydrogenation of ethylbenzene). The mechanism included both the adsorption of hydrogen and toluene and the sequential addition of hydrogen to toluene in three consecutive surface reaction steps, where the surface intermediates conserved their aromatic nature. The model, assuming the adsorption of toluene and hydrogen on different sites, involves the following steps:

$$H_2 + * \overset{K_H}{\rightleftharpoons} \gamma H_{2/\gamma}* \tag{8}$$

$$T + S \overset{K_T}{\rightleftharpoons} TS \tag{9}$$

$$TS + \gamma H_{2/\gamma}* \overset{K_H}{\underset{k_{-1}}{\rightleftharpoons}} TH_2S + \gamma* \tag{10}$$

$$TH_2S + \gamma H_{2/\gamma}* \overset{k_2}{\underset{k_{-2}}{\rightleftharpoons}} TH_4S + \gamma* \tag{11}$$

$$TH_4S + \gamma H_{2/\gamma}* \overset{k_3}{\underset{k_{-3}}{\rightleftharpoons}} TH_6S + \gamma* \tag{12}$$

$$TH_6S \overset{rapid}{\longrightarrow} TH_6 + S \tag{13}$$

Here $\gamma = 1$ for molecular adsorption of hydrogen and $\gamma = 2$ for dissociative adsorption. The same equations can be used to describe the competitive adsorption of hydrogen and toluene by setting S = *. The additional
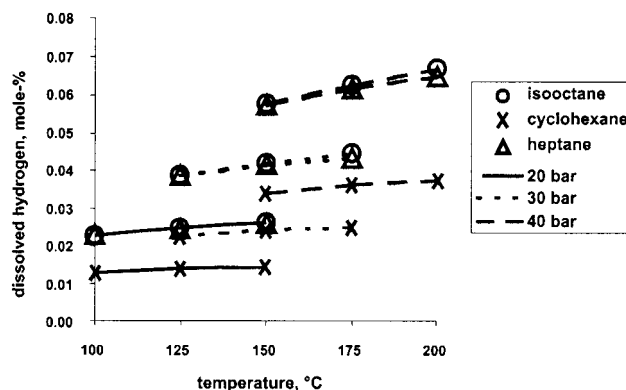

Figure 6. Hydrogen solubility in isooctane, *n*-heptane, and cyclohexane at different pressures and temperatures.
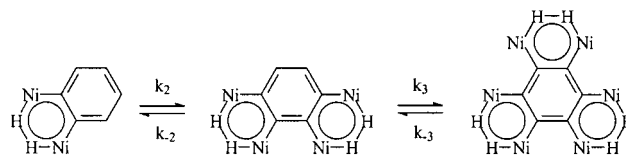

Figure 7. Principle of formation of intermediates in benzene ring hydrogenation.

assumption of toluene adsorption on multiple sites was achieved by setting S = X*. Surface reactions, (10)–(12), were presumed to be rate-determining steps, whereas adsorption of both hydrogen and toluene was rapid. The number of parameters was reduced by assuming equal and irreversible hydrogenation steps ($k_1 = k_2 = k_3 = k$ and $k_{-1} = k_{-2} = k_{-3} = 0$). The rate equation for the competitive adsorption of toluene and hydrogen was then simplified to

$$r = kK_TK_Hc_Tc_H\Theta_V^{\gamma+X} \tag{14}$$

$$\Theta_V[1 + (K_Hc_H)^{1/\gamma}] + \Theta_V^X(3K_Tc_T) = 1 \tag{15}$$

and for the noncompetitive adsorption to

$$r = \frac{kK_TK_Hc_Tc_H}{[1 + (K_Hc_H)^{1/\gamma}]^\gamma(1 + 3K_Tc_T)} \tag{16}$$

Note that similar rate equations would be achieved even without assuming the aromatic nature of the intermediates (by applying the theory of kinetic coupling[15]).

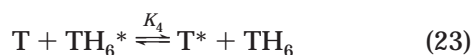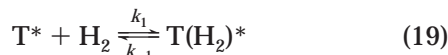Arrhenius' law was applied to the temperature dependence of the rate constant k

$$k = k(T_{ref}) \exp\left[-\frac{E_a}{R}\left(\frac{1}{T} - \frac{1}{T_{ref}}\right)\right] \tag{17}$$

As a first assumption, adsorption coefficients K_T and K_H were presumed to be temperature independent. At a later stage, the temperature dependence was modeled with the van't Hoff equation

$$K = e^{S/R}e^{-\Delta H/RT} \tag{18}$$

Temkin et al.[13] have described an alternative mechanism where the adsorbed aromatic compound forms a naphthalene-type intermediate with physisorbed hydrogen [T(H₂)*]. In accordance with the same principle, the second step gives a phenanthrene-type intermediate complex, which reacts to cyclohexene and finally to

cyclohexane. The reaction steps can be described as follows:

$$T^* + H_2 \underset{k_{-1}}{\overset{k_1}{\rightleftharpoons}} T(H_2)^* \tag{19}$$

$$T(H_2)^* + H_2 \underset{k_{-2}}{\overset{k_2}{\rightleftharpoons}} T(H_2)_2^* \tag{20}$$

$$T(H_2)_2^* \overset{k_3}{\longrightarrow} TH_4^* \qquad \text{rds} \tag{21}$$

$$TH_4^* + H_2 \overset{\text{rapid}}{\longrightarrow} TH_6^* \tag{22}$$

$$T + TH_6^* \overset{K_4}{\rightleftharpoons} T^* + TH_6 \tag{23}$$

A quasi-steady state was assumed for the surface components and quasi-equilibrium for the desorption stage (eq 23). The mechanism was further simplified by assuming irreversible complex formation ($k_{-1} = k_{-2} = 0$). To reduce the number of parameters to an acceptable level, it was necessary to assume as well that the reaction rate was much greater in one or the other of the first two reaction steps (i.e., $k_1 \gg k_2$ or $k_1 \ll k_2$). The two approximations would simplify the rate equation to the same mathematical formula, and optimization would then yield the same parameter values. The mechanism behind the approximations differs, however. With $k_1 \gg k_2$ and also K_4 essentially larger than 1, coverage of the reagent would be high. In turn, $k_2 \gg k_1$ would lead to a high coverage of intermediate $T(H_2)^*$ and zero-order behavior of toluene. High coverage of intermediates or hydrogen-deficient species has been reported elsewhere,[12,22] and it was assumed here, too, leading to the simplified expression

$$r = \frac{k_2 c_T c_H}{\dfrac{k_2}{k_3} c_T c_H + \dfrac{1}{K_4} c_{TH_6} + c_T} \tag{24}$$

3.5. Hydrogenation, Parameter Estimation. Kinetic parameters were estimated by minimizing the sum of squares (RSS) of differences between the experimental and estimated liquid mole fractions. The Marquardt–Levenberg optimization method was used for the estimation, which was carried out by the in-house optimization program KINFIT. The correlation between parameters was reduced by writing eqs 14 and 16 in the form

$$r = k_{ref} e^{-E_a/R(1/T - 1/T_{ref})} \frac{c_T c_H \Theta_V^{\gamma + X}}{c_{T,ref} c_{H,ref} \Theta_{V,ref}^{\gamma + X}} \tag{25}$$

$$r = k_{ref} e^{-E_a/R[1/T - 1/T_{ref}]} \frac{c_T c_H [1 + (K_H c_{H,ref})^{1/\gamma}]^{\gamma} (1 + 3 K_T c_{T,ref})}{c_{T,ref} c_{H,ref} [1 + (K_H c_H)^{1/\gamma}]^{\gamma} (1 + 3 K_T c_T)} \tag{26}$$

where reference concentrations and temperature, $c_{T,ref}$, $c_{H,ref}$, and T_{ref}, were defined as average values 1160 and 230 mol/m³ and 128.85 °C (400 K), respectively.

A heterogeneous reactor model (eqs 3–7) was first tested with the Smeds model (eqs 15 and 25), assuming dissociative adsorption of hydrogen and that adsorbed toluene occupies one site. Adsorption coefficients K_T and
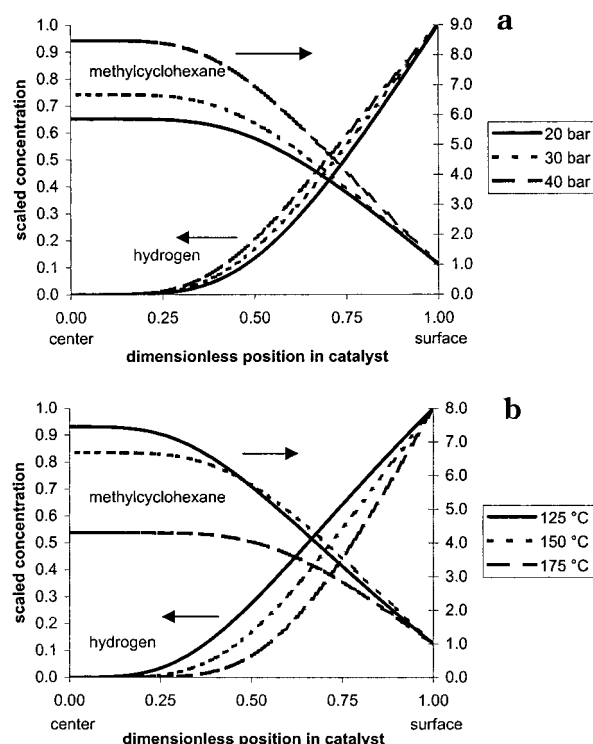
Figure 8. (a) Concentration profiles inside the catalyst particle in toluene hydrogenation in isooctane at 150 °C, toluene concentration of 25 mol %, and different pressures. (b) Concentration profiles inside the catalyst particle in the toluene hydrogenation in isooctane at 30 bar, toluene concentration of 25 mol %, and different temperatures.

K_H were presumed to be temperature independent. Relative concentration profiles of hydrogen and methylcyclohexane within the catalyst particle are illustrated in Figure 8a,b. As can be seen, pressure did not have as marked effect on the concentration profiles as temperature. A steep decrease in the hydrogen concentration suggests a strong intraparticle mass-transfer resistance. However, the nonlinear dependence of the hydrogen concentration in the formation of methylcyclohexane (see Figure 8a) and the exponential dependence of temperature (see Figure 8b) indicate that the hydrogenation rate was determined not only by the mass transfer but also by the chemical kinetics. The toluene concentration decreased typically by 10–20%, whereas no significant differences in the solvent concentration were observed inside the catalyst.

Adsorption coefficients K_T and K_H were first assumed to be temperature independent. The large confidence interval of the hydrogen adsorption coefficient suggested, however, that the assumption of temperature independence for K_H might not be valid or else that the mechanism was incorrect. In fact, both adsorption and desorption of hydrogen and aromatic compounds have proved to be strongly dependent on temperature.[5,23] Unfortunately, the estimation made with temperature-dependent adsorption coefficients gave no reasonable parameters, for either K_H or K_T, and led to a strong correlation between parameters, indicating that the temperature dependence of the adsorption coefficients could not be estimated with the present data. Poor predictability of the hydrogen adsorption coefficient encouraged us also to apply the Eley–Rideal-type mechanism (suggested also elsewhere[8,24]), where hydrogen reacts from the gas phase. The rate equation

Table 1. Kinetic Parameters (95% Confidence Interval) for Toluene Hydrogenation Assuming Dissociative Adsorption of Hydrogen, the Smeds Model

	competitive adsorption[a]	competitive adsorption[b]	noncompetitive adsorption
k_{ref}, mol/(kg h)	$9.5 \pm 0.9 \times 10^{-2}$	$9.9 \pm 0.8 \times 10^{-2}$	$8.8 \pm 0.8 \times 10^{-2}$
E_a, kJ/mol	48.8 ± 1.8	48.0 ± 1.6	50.0 ± 1.6
K_{tol}, m³/mol	$1.1 \pm 0.3 \times 10^{-4}$	$5.3 \pm 3.6 \times 10^{-4}$	$1.1 \pm 0.6 \times 10^{-3}$
K_H, m³/mol	$38.6 \pm 3.5 \times 10^{-4}$	$5.2 \pm 10.1 \times 10^{-4}$	$27.9 \pm 27.5 \times 10^{-3}$
X	1.0	7.1 ± 7.5	
RSS	1.41	1.34	1.23
RRMS	0.062	0.060	0.058

[a] Fixed X; toluene occupies one active site. [b] Adjustable X; toluene occupies X active sites.

Table 2. Kinetic Parameters (95% Confidence Interval) for Toluene Hydrogenation Assuming Molecular Adsorption of Hydrogen, the Smeds Model

	competitive adsorption[a]	competitive adsorption[b]	noncompetitive adsorption	Eley–Rideal
k_{ref}, mol/(kg h)	$9.7 \pm 0.9 \times 10^{-2}$	$10.3 \pm 0.8 \times 10^{-2}$	$8.8 \pm 0.8 \times 10^{-2}$	$13.1 \pm 0.5 \times 10^{-2}$
E_a, kJ/mol	48.5 ± 1.8	47.5 ± 1.6	49.9 ± 1.7	43.1 ± 1.3
K_{tol}, m³/mol	$1.7 \pm 0.6 \times 10^{-4}$	$3.4 \pm 1.5 \times 10^{-4}$	$1.1 \pm 0.6 \times 10^{-3}$	$3.1 \pm 1.2 \times 10^{-4}$
K_H, m³/mol	$38.0 \pm 18.4 \times 10^{-4}$	$5.7 \pm 3.7 \times 10^{-4}$	$14.9 \pm 8.5 \times 10^{-3}$	
X	1.0	12.3 ± 9.3		
RSS	1.44	1.35	1.25	1.64
RRMS	0.062	0.061	0.058	0.66

[a] Fixed X; toluene occupies one active site. [b] Adjustable X; toluene occupies X active sites.

with assumptions similar to those for eq 16 led to the formula

$$r = \frac{kK_A c_A c_H}{1 + 3K_A c_A} \qquad (27)$$

The estimated adsorption coefficients of the solvents were 1 order of magnitude lower than the coefficient of toluene, indicating that solvents did not adsorb on the catalyst. Because solvents played no role in the mechanism, all data sets could be treated together in the subsequent parameter estimation and the adsorption of solvent could be from the kinetic model. This kind of more general model has the advantage of widened applicability. The results showed that the proper approach with appropriate simplifications had been applied and, thus, intrinsic kinetics was obtained. It was concluded that the difference in the hydrogenation rates in the three solvents was primarily due to the different solubility of hydrogen.

The several variations of the Smeds model included both competitive and noncompetitive adsorption of hydrogen and toluene as well as dissociative and molecular adsorption of hydrogen. The competitive adsorption model also included the possibility that toluene occupied multiple sites, $X > 1$, as suggested in the literature.[7,11] This multiple-site case was compared with the case in which toluene occupied just one site, $X = 1$. Our results indicated that the assumption of toluene adsorption on multiple active sites is justified (Tables 1 and 2) despite the large confidence limits of these parameters. The estimated apparent activation energies were about 48–50 kJ/mol, which are in agreement with both the gas- and liquid-phase hydrogenations of aromatic compounds.[4,5,9,10,12] However, even though a decline in the catalyst activity could not be observed, it is possible that some deactivation was concealed in the data; i.e., the catalyst activity was in steady state but included some deactivation, which differed with temperature and pressure. A study of the deactivation will be included in a future paper.

All models gave a good fit and, in practice, no variation of the Smeds model could be concluded to be superior on the basis of the RSS or the residual root

mean square (RRMS). The fit for one of the Smeds model variations (dissociative adsorption of hydrogen, $\gamma = 2$, and competitive adsorption of hydrogen and toluene assuming that toluene occupied one site, $X = 1$) is illustrated in Figure 9a–c. The fit of the hydrogenation rate was excellent in isooctane (Figure 9a); the rate was slightly overestimated at elevated temperature in heptane (Figure 9b) and clearly overestimated at 200 °C in cyclohexane (Figure 9c). These overestimates could have been due to an experimental error or, alternatively, could have reflected a real decrease in rate due to the reaction maximum, which occurred at lower temperature with cyclohexane because of the lower hydrogen equilibrium concentration. The reaction orders observed at higher temperatures, 1 for hydrogen and 0 for toluene, are described by all of the competitive, noncompetitive, and Eley–Rideal-type models because the adsorption term for hydrogen, $(K_H c_H)^{1/\gamma}$, is small and, correspondingly, term $3K_T c_T$ is large in eqs 15 and 16. The rate equation is then reduced to $r = kK_H c_H$. However, with the simplifications employed, the Smeds model was not able to predict reaction orders at low temperatures.

The residual (RSS) of the Temkin model (eq 24) was about 25–35% less than the residual of the Smeds model, and the deviation (RRMS) was also lower than that for the Smeds model (Table 3). Together with the narrow confidence intervals, this indicates a better fit. The fit is illustrated in Figure 10a–c. Model deviation was similar to though smaller than that obtained with the Smeds model. However, the Temkin model was able to predict the observed reaction order for both toluene and hydrogen through the entire temperature range. The term including the methylcyclohexane concentration could be ignored because $K_4^{-1} c_{TH_6}$ is very low in all conditions, i.e., $K_4^{-1} c_{TH_6} \ll c_T$ and $(k_2/k_3) c_T c_H$ (very low conversion of toluene). The rate eq 24 was then reduced to

$$r = \frac{k_2 c_H}{\dfrac{k_2}{k_3} c_H + 1} \qquad (28)$$

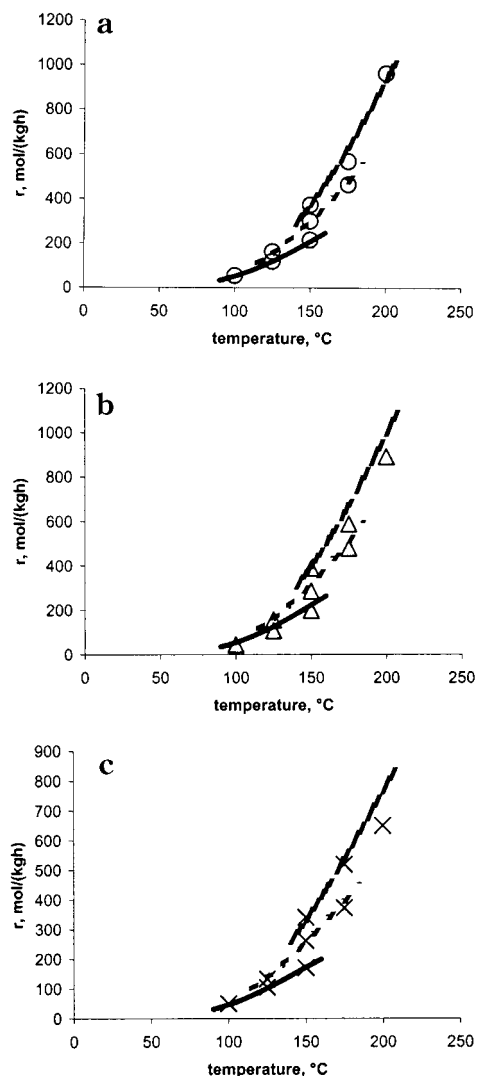At low temperatures, the term $(k_2/k_3) c_H$ is much greater

Figure 9. (a) Fit of the Smed model (eq 14; $\gamma = 2$, $X = 1$); toluene hydrogenation rate in isooctane. (b) Fit of the Smed model (eq 14; $\gamma = 2$, $X = 1$); toluene hydrogenation rate in n-heptane. (c) Fit of the Smed model (eq 14; $\gamma = 2$, $X = 1$); toluene hydrogenation rate in cyclohexane.

Table 3. Kinetic Parameters (95% Confidence Interval) for Toluene Hydrogenation, the Temkin Model

	Temkin model (eq 24)	simplified Temkin model (eq 28)
k_2, mol/(kg h)	$1.9 \pm 0.4 \times 10^{-3}$	$2.3 \pm 0.7 \times 10^{-3}$
k_3, mol/(kg h)	0.22 ± 0.07	0.11 ± 0.02
E_{a2}, kJ/mol	32.6 ± 4.7	17.4 ± 5.1
E_{a3}, kJ/mol	82.2 ± 7.5	69.6 ± 4.2
K_4	0.12 ± 0.04	
RSS	0.91	1.14
RRMS	0.050	0.055

than 1, leading to zero-order behavior ($r = k_3$), as was observed. At higher temperatures, the term $(k_2/k_3)c_H$ is much less than 1, leading to the first-order reaction ($r = k_2 c_H$). The fit of the rate equation (28) (the simplified Temkin model) was slightly better than the fit of the Smeds models but a bit poorer than the fit of the rate equation (24) (the Temkin model; see Table 3).

4. Conclusions

Toluene hydrogenation in isooctane, n-heptane, and cyclohexane was studied in a three-phase reactor. The
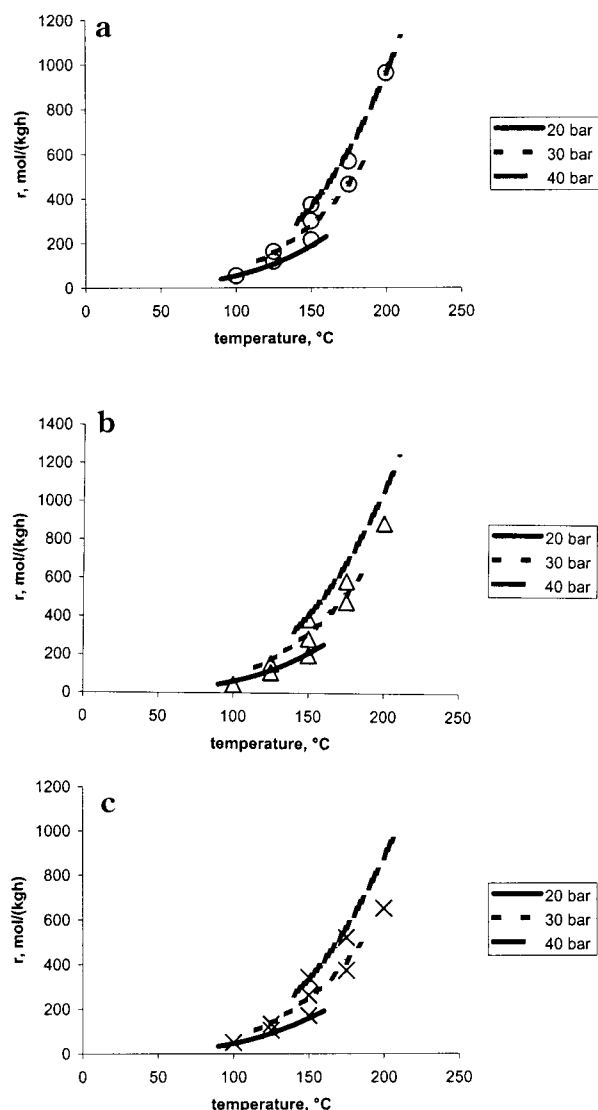

Figure 10. (a) Fit of the Temkin model (eq 24); toluene hydrogenation rate in isooctane. (b) Fit of the Temkin model (eq 24); toluene hydrogenation rate in n-heptane. (c) Fit of the Temkin model (eq 24); toluene hydrogenation rate in cyclohexane.

steady-state hydrogenation rate increased with both temperature and pressure. The rates in isooctane and heptane were similar, whereas the rate in cyclohexane was lower, particularly at elevated temperatures. Near zero-order reaction toward toluene with an increase in temperature and at the same time increasing reaction order toward hydrogen, from about zero to first order, were in agreement with earlier results for the group VIII metals. The GL and LS mass-transfer resistance did not have a significant effect on the hydrogenation rate, whereas the intraparticle mass transfer had a significant effect on the rate and estimated parameters.

The kinetic model that was developed included competitive adsorption of toluene and methylcyclohexane and the formation of surface intermediates by the adsorbed toluene and the liquid-phase hydrogen. Intermediates were presumed to retain their aromatic nature. In a third step the phenanthrene-type surface complex was isomerized to methylcyclohexene, which was then further hydrogenated to methylcyclohexane. This model described the observed reaction orders and gave an excellent fit with physically meaningful parameters.

The difference between hydrogenation rates in the different solvents can be explained by differences in the hydrogen solubility, which followed the same trend as the hydrogenation rate. Furthermore, the estimated adsorption equilibrium coefficients of the solvents indicated that they did not adsorb on the catalyst. No other solvent effects were detected. The results obtained should be useful in the design of industrial hydrogenation applications: the derived kinetic model can be applied in reactor and process optimization.

Acknowledgment

Notation

a_{GL} = gas−liquid mass-transfer area/reactor volume, 1/m
c_i = concentration of component i, mol/m^3
$c_{L,i}^b$ = liquid bulk concentration of component i, mol/m^3
$c_{L,i}^p$ = liquid concentration of component i in the particle, mol/m^3
c_T = toluene concentration, mol/m^3
c_H = hydrogen concentration, mol/m^3
CSTR = continuous stirred tank reactor
D_i = diffusion coefficient of component i, m^2/s
$D_{i,eff}$ = effective diffusion coefficient of component i, m^2/s
E_a = apparent activation energy, kJ/mol
$F_{G,i}$ = feed of component i (gas phase), mol/s
$F_{L,i}$ = feed of component i (liquid phase), mol/s
ΔH = adsorption enthalpy, kJ/mol
J_i = diffusion flux of component i, mol/(m^{2}s)
k = reaction rate constant, mol/(kg h)
$k_{G,i}$ = gas-side mass-transfer coefficient, m/s
$k_{L,i}$ = liquid-side mass-transfer coefficient, m/s
K_i = vaporization equilibrium coefficient of component i
K_H = adsorption equilibrium constant for hydrogen, m^3/mol
K_T = adsorption equilibrium constant for toluene, m^3/mol
LHSV = liquid hourly space velocity (per liquid volume in reactor), 1/h
m_{cat} = catalyst mass, kg
$N_{GL,i}$ = mass-transfer flux of component i at the gas−liquid interface, mol/(m^2 s)
r = reaction rate, mol/(kg h)
r_i = generation rate, mol/(kg h)
r_{app} = apparent reaction rate, mol/(kg h)
R = gas constant, 8.314 J/(mol K)
R_p = catalyst particle radius, m
S = eq 11 adsorption entropy, J/(mol K)
S = active site (on the catalyst) occupied by toluene
T = temperature, K
V_R = reactor volume, m^3
x = dimensionless position in the catalyst
X = number of active sites (on the catalyst) occupied by toluene

Sub- and Superscripts

b = bulk
i = gas−liquid interface
p = catalyst particle

Greek Letters

ϵ = porosity of the catalyst
γ = active sites occupied by the hydrogen molecule, 1 for molecular adsorption and 2 for dissociative adsorption
Θ_V = free (fractional) vacant sites on the catalyst
ρ_p = particle density of the catalyst, kg/m^3
τ = tortuosity of the catalyst

Literature Cited

(1) Walsh, M. Motor Vehicle Pollution Control. *Platinum Met. Rev.* **2000**, *44*, 22.

(2) Karonis, D.; Lois, E.; Stournas, S.; Zannikos, F. Correlation of Exhaust Emissions from Diesel Engine with Diesel Fuel Properties. *Energy Fuels* **1998**, *12*, 230.

(3) Cooper, B.; Donnis, B. Aromatic Saturation of Distillates: An Overview. *Appl. Catal. A* **1996**, *137*, 203.

(4) Toppinen, S.; Rantakylä, T.-K.; Salmi, T.; Aittamaa, J. Kinetics of the Liquid-Phase Hydrogenation of Benzene and Some Monosubstituted Alkylbenzenes over a Nickel Catalyst. *Ind. Eng. Chem. Res.* **1996**, *35*, 1824.

(5) Singh, U.; Vannice, M. Kinetic and Thermodynamic Analysis of Liquid-Phase Benzene Hydrogenation. *AIChE J.* **1999**, *45*, 1059.

(6) Stanislaus, A.; Cooper, B. Aromatic Hydrogenation Catalysis: Review. *Catal. Rev.−Sci. Eng.* **1994**, *36*, 75.

(7) Lindfors, L. P.; Salmi, T. Kinetics of Toluene Hydrogenation on a Ni/Al₂O₃ Catalyst. *Ind. Eng. Chem. Res.* **1993**, *32*, 34.

(8) Karanth, N.; Hughes, R. The Kinetics of the Catalytic Hydrogenation of Toluene. *J. Appl. Chem. Biotechnol.* **1972**, *23*, 817.

(9) Meerten, R.; Coenen, J. Gas Phase Benzene Hydrogenation on a Nickel-Silica Catalyst. *J. Catal.* **1975**, *37*, 37.

(10) Franco, H.; Phillips, M. Gas Phase Hydrogenation on Supported Nickel Catalyst. *J. Catal.* **1980**, *63*, 346.

(11) Smeds, S.; Murzin, D.; Salmi, T. Kinetics of Ethylbenzene Hydrogenation on Ni/Al₂O₃. *Appl. Catal. A* **1995**, *125*, 271.

(12) Lin, S.; Vannice, M. Hydrogenation of Aromatic Hydrocarbons over Supported Pt Catalysts. *J. Catal.* **1993**, *143*, 563.

(13) Temkin, M.; Murzin, D.; Kulkova, N. Mechanism of the Liquid-Phase Hydrogenation of the Benzene Ring. *Kinet. Katal.* **1989**, *30*, 637.

(14) Smeds, S.; Murzin, D.; Salmi, T. On the Kinetic Coupling and Mechanism of the Aromatic Ring Hydrogenation. *React. Kinet. Catal. Lett.* **1998**, *63*, 47.

(15) Boudart, M. Thermodynamic and Kinetic Coupling of Chain and Catalytic Reactions. *J. Phys. Chem.* **1983**, *87*, 2786.

(16) Miller, D. Scale-Up of Agitated Vessels Gas−Liquid Mass Transfer. *AIChE J.* **1974**, *20*, 445.

(17) Weisz, P.; Prater, C. Interpretation of Measurements in Experimental Catalysis *Adv. Catal.* **1954**, *6*, 143.

(18) Damkoehler, G. Übertemperatur in Kontaktkörnern. *Z. Phys. Chem.* **1943**, *193*, 16.

(19) Reid, R.; Prausnitz, J.; Poling, B. *The Properties of Gases and Liquids*; McGraw-Hill Book Co.: New York, 1987; p 741.

(20) Satterfield, C. *Mass Transfer in Heterogeneous Catalysis*; MIT Press: Cambridge, MA, 1970; pp 38−39.

(21) Aittamaa, J.; Keskinen, K. Flowbat−User's Instruction Manual; Laboratory of Chemical Engineering, Helsinki University of Technology, Finland 2000.

(22) Lafyatis, D.; Creten, G.; Dewaele, O.; Froment, G. A Simple Method of Estimating Surface Reaction Rates by Moment Analysis of TAP Reactor Pulse Experiments: Application to Benzene Hydrogenation. *Can. J. Chem. Eng.* **1997**, *75*, 1100.

(23) Smeds, S.; Salmi, T.; Lindfors, L. P.; Krause, O. Chemisorption and TPD Studies of Hydrogen on Ni/Al₂O₃. *Appl. Catal.* **1996**, *144*, 177.

(24) Kehoe, J.; Butt, J. Kinetics of Benzene Hydrogenation by Supported Nickel at Low Temperature. *J. Appl. Chem. Biotechnol.* **1972**, *22*, 23.